TIME2IMAGE: A UNIFIED ADAPTIVE IMAGE REPRESENTATION FRAMEWORK FOR TIME SERIES CLASSIFICATION

Anonymous authors
Paper under double-blind review

ABSTRACT

Time Series Classification (TSC) is a crucial and challenging task that holds significant importance across various domains, of which one of the kernel ingredients is to construct a suitable time series representation for better feature capture. However, extracting informative and robust time series representation with good generalization potential is still a challenging problem. To address this issue, we propose Time2Image, a novel image-based representation framework for TSC. At the heart of our framework is a proposed Adaptive Time Series Gaussian Mapping (ATSGM) module for robust time series encoding in 2D image structure, based on which we employ Vision Transformer (ViT) for subsequent classification tasks considering its prominent long-dependency modeling capability. Experiments were conducted on all 158 public time series datasets from UCR/UEA covering diverse domains, among which our method achieves top 1 performance in 86 datasets compared with existing State-Of-The-Art (SOTA) deep learning-based methods. In addition, our framework flexibly allows handling both univariate and multivariate time series with unequal length across different domains and takes inherent advantage of generalization ability due to our proposed ATSGM representation method. The source code will be publicly available soon.

1 INTRODUCTION

Time series classification (TSC) is recognized as a classic but challenging task in data mining (Esling & Agon, 2012), which aims to assign predefined labels to chronologically arranged data of both Univariate Time Series (UTS) and Multivariate Time Series (MTS) according to the number of channels of the sample. It can be widely applied across diverse fields in finance(Xiu et al., 2021; Chao et al., 2019), healthcare(Chambon et al., 2018), transportation(Gupta et al., 2020), etc. Over the past few years, TSC algorithms can be mainly concluded into 3 categories:(i) Traditional machine learning models(Formisano et al., 2008; Bagnall et al., 2017) use various feature extraction techniques for statistic(Lin et al., 2012; Li et al., 2018), frequency(Baydogan et al., 2013), sequence(Chen et al., 2021) or shapelet(Ye & Keogh, 2009; Grabocka et al., 2014) feature capturing combined with traditional classification methods(Xue et al., 2019) like SVM, KNN, etc. (ii) Deep learning models(Chen & Shi, 2019; Ruiz et al., 2021) have automatic feature learning ability through neural network models to achieve more substantial expressive power compared with traditional methods. Typical algorithms for sequence modeling ability including RNN, LSTM, especially Transformer-related models based on attention mechanism on long-term dependencies capturing. (iii) Ensemble models(Lines et al.) integrate the results by combining multiple base classifiers to improve classification performance. However, existing algorithms are only suitable for either UTS or MTS with heavy feature engineering and hyperparameter tuning, which brings subjectivity to the model.

Unlike the above models which extract time series representation based on original time series data, in recent years, increasing attention has been focused on transformation-based time series representation(Bagnall et al., 2012). These methods model time series data with specific data structure for informative feature extraction, among which time series image representation has become one of the active areas in recent years with the rapid development and achievements of image classification algorithms in computer vision(Chen & Shi, 2019). The motivation behind image representation is to convert time series into images to reformat the data for effective pattern detection to strengthen

the expressive power of the data by leveraging experience in image feature extraction. However, current image representation methods suffer from poor generalization, which can be reflected in two aspects: from the data perspective, current approaches are only effective in specific time series datasets or in certain domains; from the model perspective, existing image representation methods cannot be applied to both UTS and MTS. Even though some models can be adopted on MTS, many of them cannot be used when the lengths of time series are inconsistent. Therefore, our goal of this work is to propose a novel time series image representation framework that not only has a better comprehensive performance compared with existing deep learning SOTA algorithms but also has the inherent generalization ability to both UTS and MTS with inconsistent length.

In this paper, we proposed a unified adaptive image representation framework for time series classification called Time2Image. In our framework, Adaptive Time Series Gaussian Mapping (ATSGM) is first introduced to convert time series into an image consisting a collection of mixed Gaussian images where the image number equals the length of the time series data. Moreover, each mixed Gaussian image is jointly constructed based on a specific two-dimensional Gaussian distribution and the values of the time series data at a certain time point. By converting the projection of the time series data into an 'equal circle in a square' problem, the optimal value of the specific Gaussian distribution parameters and the position of each channel in the image can be obtained given channel number and image size. After that, the time series classification is converted into an image classification problem, and the vision transformer algorithm is adopted with the help of its long-term dependency-capturing ability. This design enables spatial structure construction of time series through image representations and can be generalized to both UTS and MTS with unequal lengths. Overall, the contributions can be summarized as follows:

- Adaptive Time Series Gaussian Mapping (ATSGM) module is proposed for robust time series encoding in 2D images, which can be generalized to both UTS and MTS.
- The vision transformer adopted in Time2Image is the first attempt at a time series classification task.
- We validate the effectiveness of our approach based on all 158 public datasets from UCR/UEA. Experimental results show that our approach achieves notably superior performance compared with SOTA baselines.

2 Related Work

2.1 Time series Transformation Methods

With the accumulation of time series data in various domains, transforming time series into alternative representations has become crucial for advanced analysis tasks as a way to improve the expressive power of original data(Lacasa et al., 2015)(Meintjes et al.). Graph-based transformation method is a flexible framework to capture complex interrelationships and dependencies within a time series(Cheng et al., 2020). Techniques such as Visibility graph(Xiu et al., 2022), Recurrence network(Donges et al., 2012), and Transition network (Makaram et al., 2021) are available for time series modeling. Under this framework, graph theory and network science can be adopted for further tasks but constructing a graph is computationally expensive, especially for long time series data. Moreover, symbolic sequence representation aims to simplify continuous time series data into discrete symbols based on predefined rules. A Method like Symbolic Aggregation approXimation (SAX)(Senin & Malinchik, 2013) is proposed for representation, which allows the utilization of symbolic analysis, but it will inevitably lose detailed information and the selection of the parameters is subjective. In the meantime, numerical transformation includes Fourier Transform(Zhao et al., 2017), Wavelet Transform(Chaovalit et al., 2011), etc. endeavor to execute mathematical operations for spectral component capturing or features from different scales, but the estimation and selection of suitable transformation functions can also be subjective.

In addition to the above methods, image-based representation has gained popularity in recent years with the development of computer vision. Existing image-encoder methods (Li et al., 2021; Wang & Oates, 2015; Chen & Shi, 2019) for time series include Gramian Angular Field (GAF), Markov Transition Field (MTF), Recurrence Plots (RP), etc. Phase relationships, recurrence patterns, and frequency-related features can be captured through current techniques. Since there is a significant

gap between the existing time series image representation method for classification and the SOTA models on the TSC task, we propose a new time series image representation method in this paper.

2.2 IMAGE CLASSIFICATION

When it comes to image classification, various deep learning architectures have emerged as state-of-the-art models for image classification. Existing architectures can be concluded into 2 categories: Convolutional Neural Networks(CNNs)(Esling & Agon, 2012; Li et al., 2021) based models and Transformer based models(Dosovitskiy et al., 2021). CNNs have revolutionized this field, achieving remarkable results by effectively capturing local spatial dependencies through convolutional layers and hierarchical features via pooling and stacking operations, of which ResNet(He et al., 2016) is a typical model of CNN-based models. More recently, attention mechanisms have gained attention in image classification research. After that, the emergence of ViT from Google proposed in 2021(Dosovitskiy et al., 2021) indicates that the transformer-based models have officially entered the field of image classification. However, ViT has never been applied to TSC tasks before. Since it has a good long-dependence modeling capability, it should have great potential to be applied to temporal data. In this work, by converting time series into image, we transform the time series classification into image classification and utilize vision transformer for further tasks.

3 PRELIMINARY

Let $\chi_N = \left\{X_D^N\right\}_{d=1}^D$ be the N^{th} multivariate time series data with the dimension of D. $X_D \in \mathbb{R}^{D\times T}$ refers to the D^{th} channel of time series and $X_D = \{x_{d_1,1}, x_{d_2,2}....., x_{d,t}\}$. For $\forall\chi$, D and T represent the channel and the length of the time series, respectively. Let $Y_N \in \mathbb{N}^{\mathbb{K}}$ be the corresponding label of the N^{th} sample of the time series, where K indicates the number of classes. All channels in X_N share the same label Y. We choose the definition of multivariate time series as the general definition of both univariate and multivariate time series data since univariate time series can be regarded as the special case of multivariate ones when $D = 1$. In this study, we focus on time series classification by transforming the original time series into an image (Time2Image). Our Time2Image consists of two stages: Adaptive Time Series Gaussian Mapping (ATSGM) for image representation and classification.

Definition 1 Patch. A patch refers to a small rectangular or square region extracted from the input image, which can be mathematically represented as a matrix or a vector. It is a fundamental unit in computer vision, which plays a vital role in local feature encoding and analysis. In addition, the shape and size of the patch are adaptable based on the application and models we adopt, of which smaller patches reflect fine-grained details while larger patches encompass a broader context. In this work, the patch P_t is defined as the image representation of the time series at time t, which is a 16×16 matrix since the classification method we adopt is ViT-B/16.

Definition 2 Sub-patch. A sub-patch is defined as the subsection of the patch in definition 1. As for MTS, the image representation of the time series in one channel is a sub-patch. Therefore, the number of sub-patch of a MTS sample equals the number of channels. Therefore, UTS can be regarded as a special case of MTS, of which the sub-patch and patch are the same.

4 TIME2IMAGE FRAMEWORK

In this section, a novel time series image representation framework is introduced for time series modeling. We name the proposed framework as Time2Image, which transforms time series into an image. The framework can be seen in Figure 1, from which we use D=6 as an example.

4.1 DATA PREPROCESSING

Data preprocessing plays a critical role in preparing the time series data for classification tasks. In this framework, the data preprocessing involves two techniques, which are standardization and resizing. For time series data of each channel in MTS, standardization is first conducted separately to align data to a common scale and distribution so as to ensure different time series from different

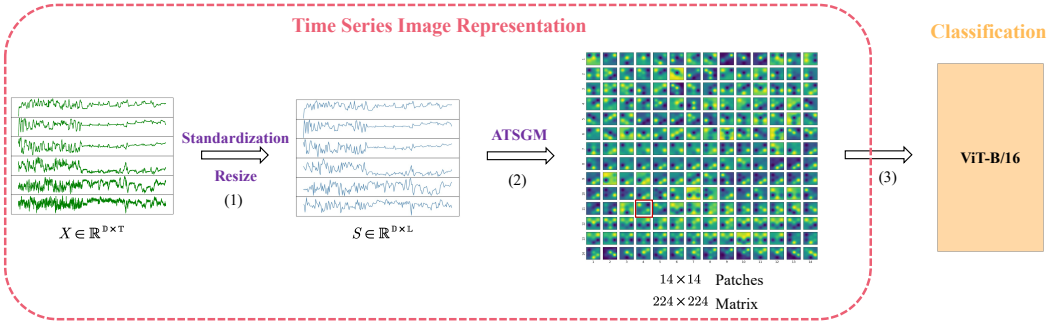

Figure 1: Time2Image Framework (1)Pre-processing: use standardization and resize to let MTS to equal-length MTS and L=196 (2) ATSGM:Gaussian mapping to model time series into a mixed Gaussian distribution as image representation (3) Use the image generated from ATSGM for image classification task

channels are comparable.

$$S_{D,T}^{N} = \frac{X_{D,T}^{N} - \mu_{X_D^N}}{\sigma_{X_D^N}} \tag{1}$$

where μ and σ are the mean and standard deviation of the time series, respectively. After that, cubic interpolation is adopted for each channel to deal with varying sequence lengths within the time series to create a consistent representation. Since the estimation process is determined through smooth cubic polynomial, it provides more accurate results, especially for complex time series data with nonlinear variations compared to simpler interpolation methods such as linear interpolation and quadratic interpolation.

4.2 Adaptive Time Series Gaussian Mapping (ATSGM)

ATSGM is a crucial component of our proposed framework for time series image representation, which addresses the challenge of extracting informative and robust representations from time series data with the goal of achieving better feature capture. Our goal is to obtain an image representation of the corresponding values of all channels at a certain time. The overall process of ATSGM can be shown in Figure 2, which involves transforming the time series at a certain time with different channels into a sequence of mixed Gaussian distributions ordered by sequence. These distributions are then used to create a sub-patch representation, where the mean and standard deviation of the Gaussian distribution correspond to the specific value through mathematical derivation based on the number of channels of MTS, which is illustrated in Section 4.2.1. The summation of the sub-patch representation is conducted and the patch representation is reached for time series at time t. All obtained patches are arranged in chronological order into 16×16 patches as the image representation of MTS as the input for the image classification algorithm. The intuition of the ATSGM is to preserve the statistical properties of time series through Gaussian distributions and obtain a smooth two-dimensional representation. The following subsection will give a detailed description of the method.

4.2.1 Time Series Image Representation

Existing research on image representation mainly considers the relative value by simply getting the difference between different time steps, but here we consider a two-dimensional Gaussian distribution in which the covariance matrix is zero in default and the two standard deviations are equal. Therefore, the projection of this Gaussian distribution is a circle in the plane, where the radius of the circle equals the standard deviation of the Gaussian distribution. Moreover, the mean μ_x and μ_y can be regarded as the coordination of the center of the circle. After that, the projection value of 2D Gaussian distribution is constructed as the sub-patch matrix, of which the length and size of the patch are predefined as a 16×16 matrix with the length of each patch equals 6, and the value is defined in a range [-3,3]. The value of the fundamental Gaussian distribution for the sub-patch matrix can be obtained through the following equation.

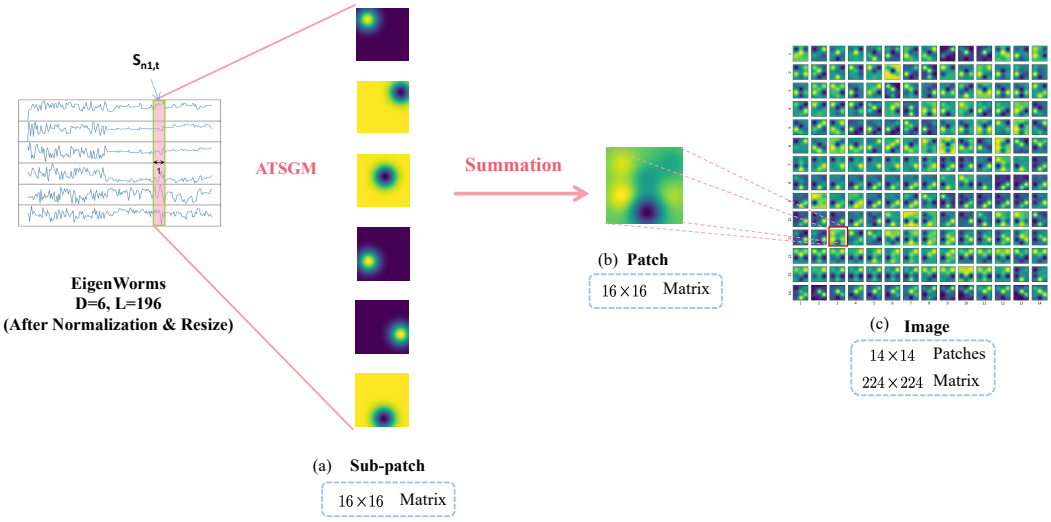

Figure 2: Time series image representation (a)Sub-patch: For pre-processed multivariate time series data, use ATSGM to get gaussian mapping of each channel at a certain time stamp (b)Patch: Do summation of sub-patch from all channels at a certain time stamp to get the patch at a certain time stamp (c) Image: Patches combined with position encoding connected in chronological order to get the final image

$$f(x,y) = \frac{1}{2\pi\sigma^2} \exp\left[-\frac{1}{2}\left(\frac{(x-\mu_x)^2}{\sigma^2} + \frac{(y-\mu_y)^2}{\sigma^2} - \frac{2(x-\mu_x)(y-\mu_y)}{\sigma^2}\right)\right] \tag{2}$$

Where $f(x,y)$ stands for the matrix value at (x,y), μ_x,μ_y and σ refers to the mean and standard deviation of the distribution, respectively. Since the projection of 2D Gaussian distribution is a circle in the plane, the relationship between the area of the circle and the standard deviation of Gaussian distribution can be derived as:

$$S_{circle} = \pi R_d^2 = \pi(\sigma)^2 \tag{3}$$

where R_D is the radius of the circle in a D-channel times series, from which we can obtain that the radius equal to the standard deviation of 2D Gaussian distribution. Here adaptive from ATSGM refers to the adjustable of the standard deviation, that is to say, we can get the representation with different information by setting different values of standard deviation. The smaller the standard deviation, the more information is captured from Gaussian mapping. According to '$3sigma$' principle, we can derive the corresponding relationship between R_D and the value of standard deviation as follows:

- When $\sigma = R_D$, about 68% of the information can be represented within the circle.
- When $\sigma = R_D/2$, about 95% of the information can be represented within the circle.
- When $\sigma = R_D/3$, about 99% of the information can be represented within the circle.

Therefore, the projection value $V_{d,t}$ of channel d at time t in the coordination of sub-patch matrix (x,y) is defined as:

$$V_{d,t}(x,y) = f(x,y) \times S_{d,t} \tag{4}$$

Where $S_{d,t}$ is the preprocessed time series value at time t. After the calculation of all data points, the characteristic of the randomness of the time series data point for each channel can be captured. Here we use the Gaussian distribution to describe the randomness of the value, adjust the range and strength of the Gaussian distribution by multiplying the normalized specific value of the time series data, and use the adjusted distribution of each dimension as the binary value under timestep dimensional representation to improve the stability and robustness of the method.

4.2.2 SUB-PATCH POSITION DETERMINATION

From the construction process of ATSGM above, we can conclude that for UTS, the optimal time series image representation can be obtained when the center of the projected circle is located at the center of the sub-patch and the diameter equals the length of the sub-patch. However, when it comes to MTS, the projection position needs to be determined first for each channel. Since the projection of 2D Gaussian distribution is a circle in the plane, we can regard it as a packing problem, which is to find the best packings of equal circles in a square. In fact, the "equal circle in a square" is a mathematical puzzle that involves finding the largest possible circle that can fit inside a given square, such that the circle's diameter is equal to the side length of the square. In other words, the goal is to determine the maximum-sized circle that can be inscribed within the square. Website[1] shows the best-known packings of equal circles in a square from N=1 to 10000, including the optimal radius (r_d) and the corresponding coordinates (c_d) of each circle given N when the length of the square is 1. In our work, N equals the number of channels in MTS. Therefore, the radius and coordinates can be obtained as:

$$R_d = r_d \times 6 \tag{5}$$

$$C_d = (c_{dx} \times 6, c_{dy} \times 6) \tag{6}$$

After finding out the optimal radius of the patch, the optimal parameters of Gaussian distribution can be determined, of which the μ_x and μ_y equal the coordinates from Equation 6, and the standard deviation can also be obtained through Equation 3. After the determination of the parameters, the distribution of Gaussian will be finally determined for each sub-patch representation. The patch representation of time step t is achieved by summing all sub-patch representations at a certain time step, which is shown in Equation 6. The image representation is the arrangement of different Patches ordered by sequence.

$$P_t(x, y) = \sum_d V_{d,t}(x, y) \tag{7}$$

The pseudo-code of ATSGM can be seen in Algorithm 1 for better understanding. Through the above steps, ATSGM is able to convert time series data into an image representation with spatial structure. This image representation can better capture the characteristics of time series data, especially the local characteristics of different channels of time series at the same time point, and provide more reliable input for subsequent image-based models.

Algorithm 1 ATSGM

Input: time series $X = [X^1, X^2, ..., X^D]$ consists of D different channel with $X^D = [x_1^D, x_2^D, ..., x_t^D]$, where x_i^D is the value of variable D at time step i and the time series length is t

Output: a 224×224 matrix N

Resize the Time Series & Normalization
For every variable, resize its length to 196: $X^{D\times T} \rightarrow X^{D\times 196}$
Transformation
Initialize P as an empty matrix with the shape of $D \times 196 \times 16 \times 16$, generate the gaussian matrix list $\Phi^{D\times 16\times 16}$ according to the number of variable D
for $i \in D$ **do**
  for $j \in L$ **do**
    $P_j^i = X_j^i \cdot \Phi_i$
  end for
end for
Reshape P
$P^{D\times 224\times 224} \leftarrow P^{D\times 196\times 16\times 16}$
Suppression P **in the dimension-0**
$P^{224\times 224} \leftarrow P^{D\times 224\times 224}$

[1] http://hydra.nat.uni-magdeburg.de/packing/csq/csq.html

4.3 CLASSIFICATION MODEL

Vision Transformer is a classical transformer-based image classification algorithm proposed in 2021(Dosovitskiy et al., 2021), which is prominent for its global feature extraction and long-dependency modeling capability because of multi-head attention. In our work, we adopt ViT-B/16 to do the image classification task with the input from our proposed time series image representation.

5 EXPERIMENT

5.1 EXPERIMENTAL SETTING

5.1.1 DATASETS

The whole UCR/UEA archive (Chen et al., 2015) is utilized to test the performance of our proposed method, which includes 128 UTS Datasets and 30 MTS Datasets. This archive is a well-known and widely used classic public dataset in time series classification. It contains 158 time series datasets in total covering different scenarios with predefined train/test split, including 128 UTS Datasets and 30 MTS Datasets. Moreover, the number of classes in this archive ranges from 2 to 60. In addition, there are 4 MTS Datasets that have unequal lengths in different channels. The summary of these datasets can be seen in Appendix A, which shows detailed information including the size of the training and testing set, channel, length, class numbers, and domains of each dataset. By testing our algorithm on all datasets and comparing it with baseline models, the performance can be obtained for further analysis.

5.1.2 BASELINES

Several comparison algorithms including SOTA methods are deployed to show the effectiveness of the proposed model. According to Ismail Fawaz et al. (2020), as for UTS, InceptionTime, FCN and ResNet achieve top 1 performance on 69.4% of the datasets by comparing 9 deep learning models, so these models are chosen as the baseline for the UTS classification task. When it comes to MTS, we choose five state-of-the-art multivariate time series classification models as our baselines: HIerarchical VotE Collective of Transformation-based Ensembles(HIVE-COTE)(Lines et al.), Canonical Interval Forest (CIF)(Middlehurst et al., 2020), RandOm Convolutional KErnel Transform (ROCKET)(Dempster et al., 2020), InceptionTime(Ismail Fawaz et al., 2020) and ResNet(He et al., 2016). HIVE-COTE, CIF, ROCKET, and InceptionTime, which are more accurate than other classifiers experimented on in the UEA archive by Ruiz et al. (2021). To show the effectiveness of the ATSGM of our framework, we also conducted the experiment to replace our following classifier from ViT to ResNet to find out the performance of the current two typical classification architectures from computer vision.

5.1.3 IMPLEMENTATION

ViT-B/16 is adopted as the following classifier for time series image representation. Therefore, the length of all time series data equals 196 (L=196). For MTS, we set the circle area of each channel to encompass the information within a 2-standard-deviation range of the predefined 2D Gaussian distribution derived from section 3, that is to say, σ = R/2 according to section 4. Moreover, we stick to the original training and testing set split for all datasets. All the test datasets were trained for 200 epochs. In the meantime, the value of hyper-parameters from ViT is set by default according to Dosovitskiy et al. (2021). The experiment of Time2Image is replicated for 5 times of each dataset with different random seeds and the value of the random seed is 0,1,2,3 and 4.

5.1.4 EVALUATION INDICATOR

We use accuracy through 5 replicate tests and calculate the average as our evaluation indicator for performance evaluation so as to make the comparison between our proposed method and the baseline models.

5.2 PERFORMANCE ANALYSIS

We did extensive experiments on the whole UCR/UEA Archive and the experimental result will be analyzed in this section. Due to page limitations, the classification accuracy of all data sets will be fully disclosed in Appendix B. The corresponding critical difference diagrams are drawn based on the performance of each dataset, which illustrates multiple pieces of information that can help make a comparison of the performance of different algorithms on multiple datasets and are shown in Figure 3 and Figure 4. As for the performance comparison between Time2Image and baselines, it can be seen that our proposed framework has the best performance on both UTS and MTS datasets, indicating the generalization ability of the proposed algorithm. Moreover, Time2Image significantly outperforms other baselines with an average rank of 1.8945 in the UTS Dataset, which wins on 73 problems out of 128 and significantly outperforms ResNet from Table 1. In addition, the performance of MTS also achieved top 1 performance compared with other baselines.

Table 1: Number of different time series image representation algorithms

Data Type	Total #	Win_# Time2Image	Win_# FCN	Win_# ResNet	Win_# ROCKET	Win_# CIF	Win_# HIVE-COTE	Win_# InceptionTime
UTS	128	**73**	12	41				
MTS	30	**13**		3	4	3	2	5

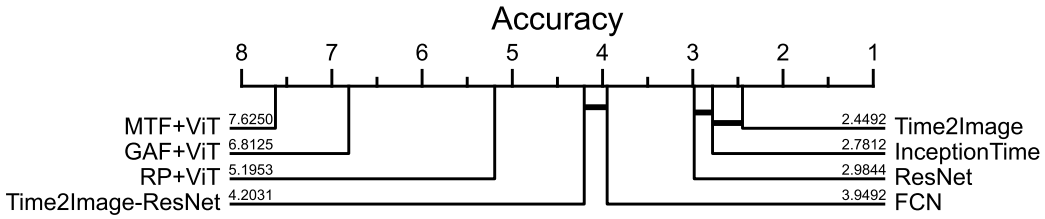

Figure 3: Critical difference diagram of UTS Dataset

Since there are some existing time series image representation methods, we also did comparison experiments on different time series image representations. GAF, MTF, and RP are universally adopted image representation methods of UTS, so we chose them for comparison, and the result can be seen in Figure 3. From the figure, it can be seen that none of the existing image representation methods can defeat baseline models. This indicates a huge research gap for time series representation for TSC, which is consistent with the current research status, but our proposed method is significantly better than not only other image representation methods but also all baselines, which provides an alternative TSC algorithm and showing a promising direction on time series image representation and providing an alternative solution on TSC task.

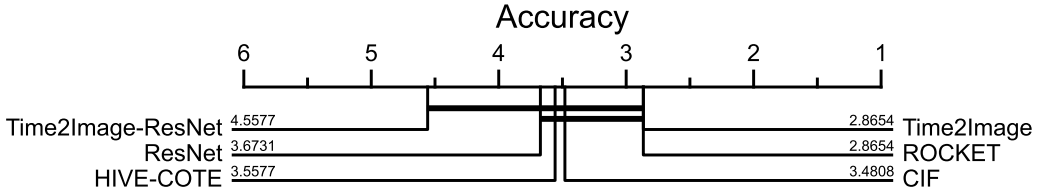

Figure 4: Critical difference diagram of MTS Dataset

In addition, to explore whether the choice of different image classification models will impact the performance, we also did an experiment on ResNet, which is a typical CNN architecture model, to replace ViT for comparison. According to the result in Figure 3, it can be seen that our proposed

framework is better than all other image representation models but not as good as SOTA, which illustrates the importance of long-range information for temporal classification and the superiority of ViT in capturing long-range information. Nevertheless, the ATSGM method we proposed still has significant advantages over other image representation learning for time series image representation, which also explains the effectiveness of our proposed ATSGM method to a certain extent.

Table 2: Classification results grouped by domains

Category	Time2Image	FCN	ResNet	Time2Image_Win	FCN_Win	ResNet_Win
Device(9)	**75.96%**	70.91%	71.16%	**4**	3	2
ECG(6)	94.67%	92.91%	**94.98%**	2	1	**3**
EOG(2)	**57.98%**	42.85%	55.06%	**1**	0	**1**
EPG(2)	99.76%	**100.00%**	**100.00%**	0	**1**	**1**
Hemodynamics(3)	**83.32%**	36.63%	62.79%	1	0	**2**
HRM(1)	**99.68%**	78.06%	98.49%	**1**	0	0
Image(32)	**83.32%**	78.16%	82.89%	**17**	1	14
Motion(17)	**81.99%**	78.03%	81.91%	**8**	2	7
Power(1)	**98.22%**	90.00%	88.89%	**1**	0	0
Sensor(30)	**84.26%**	60.73%	63.73%	**21**	1	8
Simulated(8)	94.91%	88.79%	**98.14%**	**4**	3	1
Spectro(8)	**84.67%**	66.80%	81.13%	**5**	0	3
Spectrum(4)	**79.89%**	52.44%	62.28%	**4**	0	0
Traffic(2)	**94.36%**	54.06%	54.03%	**2**	0	0
Trajectory(3)	**59.90%**	55.61%	56.33%	**2**	0	1

To test whether it can be regarded as a unified framework, performance grouped by different domains is also conducted to find out the generalization of the model. Table 2 shows the algorithms' performance with respect to the domain of the datasets. We take the domains defined by Bagnall et al. (2017) for UTS Datasets. From the table, it can be concluded that 128 datasets can be categorized into 15 domains. The first 3 columns show the average accuracy between Time2Image and baselines within the same domain and the remaining columns calculate the winning number of datasets for each model. From the table, it can be obtained that Time2Image achieves top 1 performance on 12 out of 15 domains, indicating the inherent generalization ability of Time2Image.

5.3 Parameter Analysis

From the methodology, it can be seen that our methodology is an adaptive algorithm, that is to say, the parameter, especially the value of the standard deviation(σ) of Gaussian distribution seems to have an impact on the performance. In order to explore the influence of the value of the standard deviation on the performance of the model, we record the accuracy of all data sets with different standard deviation values which can be seen in Appendix C. Here we calculate the mean of the values from Appendix C of the whole datasets to indicate the final performance of the model and the results are shown in Figure 5. From the result, it can be concluded that when $\sigma = \frac{R}{2}$, the performance of the model is the best, but the difference is not that large, of which the variance is 0.37 on average, indicating the robustness of our proposed algorithms.

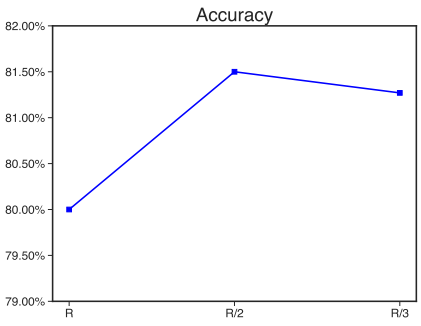

Figure 5: Parameter analysis of σ

6 Conclusion

In this work, a general time series image representation algorithm (Time2Image) was proposed, which is not only suitable for both UTS and MTS but also does a good job on non-stationary and unequal-length data. We validate the effectiveness of our approach based on all 158 public datasets from UCR/UEA. Through extensive experiments, our approach achieves notably better performance

when compared with SOTA baselines, which could be a potential solution for future time series images.

ACKNOWLEDGMENTS

We would like to express our sincere gratitude to all the reviewers and the public for your time and interest in our work. We welcome all valuable feedback and suggestions on our paper, and we think any insightful comments and constructive critiques can make this paper better.

REFERENCES

Anthony Bagnall, Luke Davis, Jon Hills, and Jason Lines. Transformation based ensembles for time series classification. In *Proceedings of the 2012 SIAM International Conference on Data Mining (SDM)*, Proceedings, pp. 307–318. Society for Industrial and Applied Mathematics, 2012. doi: 10.1137/1.9781611972825.27.

Anthony Bagnall, Jason Lines, Aaron Bostrom, James Large, and Eamonn Keogh. The great time series classification bake off: a review and experimental evaluation of recent algorithmic advances. *Data Mining and Knowledge Discovery*, 31(3):606–660, 2017.

Mustafa Gokce Baydogan, George Runger, and Eugene Tuv. A bag-of-features framework to classify time series. *IEEE Transactions on Pattern Analysis and Machine Intelligence*, 35(11):2796–2802, 2013.

Stanislas Chambon, Mathieu N. Galtier, Pierrick J. Arnal, Gilles Wainrib, and Alexandre Gramfort. A deep learning architecture for temporal sleep stage classification using multivariate and multimodal time series. *Ieee Transactions on Neural Systems and Rehabilitation Engineering*, 26(4): 758–769, 2018.

Luo Chao, Jiang Zhipeng, and Zheng Yuanjie. A novel reconstructed training-set SVM with roulette cooperative coevolution for financial time series classification. *Expert Systems with Applications*, 123:283–298, 2019.

Pimwadee Chaovalit, Aryya Gangopadhyay, George Karabatis, and Zhiyuan Chen. Discrete wavelet transform-based time series analysis and mining. *ACM Computing Surveys*, 43(2):1–37, 2011.

Wei Chen and Ke Shi. A deep learning framework for time series classification using relative position matrix and convolutional neural network. *Neurocomputing*, 359:384–394, 2019.

Yanping Chen, Eamonn Keogh, Bing Hu, Nurjahan Begum, Anthony Bagnall, Abdullah Mueen, and Gustavo Batista. The UCR time series classification archive, 2015. URL `www.cs.ucr.edu/~eamonn/time_series_data/`.

Zhi Chen, Yongguo Liu, Jiajing Zhu, Yun Zhang, Rongjiang Jin, Xia He, Jing Tao, and Lidian Chen. Time-frequency deep metric learning for multivariate time series classification. *Neurocomputing*, 462:221–237, 2021.

Ziqiang Cheng, Yang Yang, Wei Wang, Wenjie Hu, Yueting Zhuang, and Guojie Song. Time2graph: Revisiting time series modeling with dynamic shapelets. *Proceedings of the AAAI Conference on Artificial Intelligence*, 34(4):3617–3624, 2020.

Angus Dempster, François Petitjean, and Geoffrey I. Webb. ROCKET: exceptionally fast and accurate time series classification using random convolutional kernels. *Data Mining and Knowledge Discovery*, 34(5):1454–1495, 2020.

Jonathan F. Donges, Jobst Heitzig, Reik V. Donner, and Jürgen Kurths. Analytical framework for recurrence network analysis of time series. *Physical Review E*, 85(4):046105, 2012.

Alexey Dosovitskiy, Lucas Beyer, Alexander Kolesnikov, Dirk Weissenborn, Xiaohua Zhai, Thomas Unterthiner, Mostafa Dehghani, Matthias Minderer, Georg Heigold, Sylvain Gelly, Jakob Uszkoreit, and Neil Houlsby. An image is worth 16x16 words: Transformers for image recognition at scale, 2021.

Philippe Esling and Carlos Agon. Time-series data mining. *ACM Computing Surveys*, 45(1):12:1–12:34, 2012.

Elia Formisano, Federico De Martino, and Giancarlo Valente. Multivariate analysis of fMRI time series: classification and regression of brain responses using machine learning. *Magnetic Resonance Imaging*, 26(7):921–934, 2008.

Josif Grabocka, Nicolas Schilling, Martin Wistuba, and Lars Schmidt-Thieme. Learning time-series shapelets. In *Proceedings of the 20th ACM SIGKDD International conference on Knowledge discovery and data mining*, KDD '14, pp. 392–401. Association for Computing Machinery, 2014.

Ashish Gupta, Hari Prabhat Gupta, Bhaskar Biswas, and Tanima Dutta. An early classification approach for multivariate time series of on-vehicle sensors in transportation. *IEEE Transactions on Intelligent Transportation Systems*, 21(12):5316–5327, 2020.

Kaiming He, Xiangyu Zhang, Shaoqing Ren, and Jian Sun. Deep residual learning for image recognition. In *Proceedings of the IEEE Conference on Computer Vision and Pattern Recognition*, pp. 770–778, 2016.

Hassan Ismail Fawaz, Benjamin Lucas, Germain Forestier, Charlotte Pelletier, Daniel F. Schmidt, Jonathan Weber, Geoffrey I. Webb, Lhassane Idoumghar, Pierre-Alain Muller, and François Petitjean. InceptionTime: Finding AlexNet for time series classification. *Data Mining and Knowledge Discovery*, 34(6):1936–1962, 2020.

Lucas Lacasa, Vincenzo Nicosia, and Vito Latora. Network structure of multivariate time series. *Scientific Reports*, 5:15508, 2015.

Daoyuan Li, Jessica Lin, Tegawendé F Bissyandé, Jacques Klein, and Yves Le Traon. Extracting statistical graph features for accurate and efficient time series classification. pp. 12, 2018.

Taoying Li, Yuqi Zhang, and Ting Wang. SRPM–CNN: a combined model based on slide relative position matrix and CNN for time series classification. *Complex & Intelligent Systems*, 7(3): 1619–1631, 2021.

Jessica Lin, Rohan Khade, and Yuan Li. Rotation-invariant similarity in time series using bag-of-patterns representation. *Journal of Intelligent Information Systems*, 39(2):287–315, 2012.

Jason Lines, Sarah Taylor, and Anthony Bagnall. Time series classification with HIVE-COTE: The hierarchical vote collective of transformation-based ensembles. pp. 35.

Navaneethakrishna Makaram, P. A. Karthick, and Ramakrishnan Swaminathan. Analysis of dynamics of EMG signal variations in fatiguing contractions of muscles using transition network approach. *IEEE Transactions on Instrumentation and Measurement*, 70:1–8, 2021. Conference Name: IEEE Transactions on Instrumentation and Measurement.

Andries Meintjes, Andrew Lowe, and Malcolm Legget. Fundamental heart sound classification using the continuous wavelet transform and convolutional neural networks. 2018:409–412. ISSN 2694-0604. doi: 10.1109/EMBC.2018.8512284.

Matthew Middlehurst, James Large, and Anthony Bagnall. The canonical interval forest (CIF) classifier for time series classification. In *2020 IEEE International Conference on Big Data (Big Data)*, pp. 188–195, 2020.

Alejandro Pasos Ruiz, Michael Flynn, James Large, Matthew Middlehurst, and Anthony Bagnall. The great multivariate time series classification bake off: a review and experimental evaluation of recent algorithmic advances. *Data Mining and Knowledge Discovery*, 35(2):401–449, 2021.

Pavel Senin and Sergey Malinchik. SAX-VSM: Interpretable time series classification using SAX and vector space model. In *2013 IEEE 13th International Conference on Data Mining*, pp. 1175–1180, 2013. ISSN: 2374-8486.

Zhiguang Wang and Tim Oates. Imaging time-series to improve classification and imputation, 2015.

Yuxuan Xiu, Guanying Wang, and Wai Kin Victor Chan. Crash diagnosis and price rebound prediction in NYSE composite index based on visibility graph and time-evolving stock correlation network. *Entropy*, 23(12):1612, 2021.

Yuxuan Xiu, Xinyue Ren, Ting Zhang, Yanyu Chen, Li Jiang, Duo Li, Xingjun Wang, Liang Zhao, and Wai Kin Chan. Time labeled visibility graph for privacy-preserved physiological time series classification. In *2022 7th International Conference on Cloud Computing and Big Data Analytics (ICCCBDA)*, pp. 280–284, 2022.

Jiayu Xue, Xinyue Ren, Yuanjie Xu, and Qianqian Feng. Analyzing health seeking behavior of chinese residents and their influencing factors based on CHNS data. *Procedia Computer Science*, 162:835–841, 2019.

Lexiang Ye and Eamonn Keogh. Time series shapelets: a new primitive for data mining. In *Proceedings of the 15th ACM SIGKDD international conference on Knowledge discovery and data mining*, KDD '09, pp. 947–956. Association for Computing Machinery, 2009.

Bendong Zhao, Huanzhang Lu, Shangfeng Chen, Junliang Liu, and Dongya Wu. Convolutional neural networks for time series classification. *Journal of Systems Engineering and Electronics*, 28(1):162–169, 2017. Conference Name: Journal of Systems Engineering and Electronics.

A Dataset Description

A.1 Summary of UCR Univariate Datasets

Table 3: Summary of UCR Univariate Datasets

ID	Domain	Name	TrainSize	TestSize	Class	Length
1	Image	Adiac	390	391	37	176
2	Image	ArrowHead	36	175	3	251
3	Spectro	Beef	30	30	5	470
4	Image	BeetleFly	20	20	2	512
5	Image	BirdChicken	20	20	2	512
6	Sensor	Car	60	60	4	577
7	Simulated	CBF	30	900	3	128
8	Sensor	ChlorineConcentration	467	3840	3	166
9	Sensor	CinCECGTorso	40	1380	4	1639
10	Spectro	Coffee	28	28	2	286
11	Device	Computers	250	250	2	720
12	Motion	CricketX	390	390	12	300
13	Motion	CricketY	390	390	12	300
14	Motion	CricketZ	390	390	12	300
15	Image	DiatomSizeReduction	16	306	4	345
16	Image	DistalPhalanxOutlineAgeGroup	400	139	3	80
17	Image	DistalPhalanxOutlineCorrect	600	276	2	80
18	Image	DistalPhalanxTW	400	139	6	80
19	Sensor	Earthquakes	322	139	2	512
20	ECG	ECG200	100	100	2	96
21	ECG	ECG5000	500	4500	5	140
22	ECG	ECGFiveDays	23	861	2	136
23	Device	ElectricDevices	8926	7711	7	96
24	Image	FaceAll	560	1690	14	131
25	Image	FaceFour	24	88	4	350
26	Image	FacesUCR	200	2050	14	131
27	Image	FiftyWords	450	455	50	270
28	Image	Fish	175	175	7	463
29	Sensor	FordA	3601	1320	2	500
30	Sensor	FordB	3636	810	2	500
31	Motion	GunPoint	50	150	2	150
32	Spectro	Ham	109	105	2	431
33	Image	HandOutlines	1000	370	2	2709
34	Motion	Haptics	155	308	5	1092
35	Image	Herring	64	64	2	512
36	Motion	InlineSkate	100	550	7	1882
37	Sensor	InsectWingbeatSound	220	1980	11	256
38	Sensor	ItalyPowerDemand	67	1029	2	24
39	Device	LargeKitchenAppliances	375	375	3	720
40	Sensor	Lightning2	60	61	2	637
41	Sensor	Lightning7	70	73	7	319
42	Simulated	Mallat	55	2345	8	1024
43	Spectro	Meat	60	60	3	448
44	Image	MedicalImages	381	760	10	99
45	Image	MiddlePhalanxOutlineAgeGroup	400	154	3	80
46	Image	MiddlePhalanxOutlineCorrect	600	291	2	80
47	Image	MiddlePhalanxTW	399	154	6	80
48	Sensor	MoteStrain	20	1252	2	84
49	ECG	NonInvasiveFetalECGThorax1	1800	1965	42	750
50	ECG	NonInvasiveFetalECGThorax2	1800	1965	42	750
51	Spectro	OliveOil	30	30	4	570
52	Image	OSULeaf	200	242	6	427

53	Image	PhalangesOutlinesCorrect	1800	858	2	80
54	Sensor	Phoneme	214	1896	39	1024
55	Sensor	Plane	105	105	7	144
56	Image	ProximalPhalanxOutlineAgeGroup	400	205	3	80
57	Image	ProximalPhalanxOutlineCorrect	600	291	2	80
58	Image	ProximalPhalanxTW	400	205	6	80
59	Device	RefrigerationDevices	375	375	3	720
60	Device	ScreenType	375	375	3	720
61	Simulated	ShapeletSim	20	180	2	500
62	Image	ShapesAll	600	600	60	512
63	Device	SmallKitchenAppliances	375	375	3	720
64	Sensor	SonyAIBORobotSurface1	20	601	2	70
65	Sensor	SonyAIBORobotSurface2	27	953	2	65
66	Sensor	StarLightCurves	1000	8236	3	1024
67	Spectro	Strawberry	613	370	2	235
68	Image	SwedishLeaf	500	625	15	128
69	Image	Symbols	25	995	6	398
70	Simulated	SyntheticControl	300	300	6	60
71	Motion	ToeSegmentation1	40	228	2	277
72	Motion	ToeSegmentation2	36	130	2	343
73	Sensor	Trace	100	100	4	275
74	ECG	TwoLeadECG	23	1139	2	82
75	Simulated	TwoPatterns	1000	4000	4	128
76	Motion	UWaveGestureLibraryAll	896	3582	8	945
77	Motion	UWaveGestureLibraryX	896	3582	8	315
78	Motion	UWaveGestureLibraryY	896	3582	8	315
79	Motion	UWaveGestureLibraryZ	896	3582	8	315
80	Sensor	Wafer	1000	6164	2	152
81	Spectro	Wine	57	54	2	234
82	Image	WordSynonyms	267	638	25	270
83	Motion	Worms	181	77	5	900
84	Motion	WormsTwoClass	181	77	2	900
85	Image	Yoga	300	3000	2	426
86	Device	ACSF1	100	100	10	1460
87	Sensor	AllGestureWiimoteX	300	700	10	Vary
88	Sensor	AllGestureWiimoteY	300	700	10	Vary
89	Sensor	AllGestureWiimoteZ	300	700	10	Vary
90	Simulated	BME	30	150	3	128
91	Traffic	Chinatown	20	343	2	24
92	Image	Crop	7200	16800	24	46
93	Sensor	DodgerLoopDay	78	80	7	288
94	Sensor	DodgerLoopGame	20	138	2	288
95	Sensor	DodgerLoopWeekend	20	138	2	288
96	EOG	EOGHorizontalSignal	362	362	12	1250
97	EOG	EOGVerticalSignal	362	362	12	1250
98	Spectro	EthanolLevel	504	500	4	1751
99	Sensor	FreezerRegularTrain	150	2850	2	301
100	Sensor	FreezerSmallTrain	28	2850	2	301
101	HRM	Fungi	18	186	18	201
102	Trajectory	GestureMidAirD1	208	130	26	Vary
103	Trajectory	GestureMidAirD2	208	130	26	Vary
104	Trajectory	GestureMidAirD3	208	130	26	Vary
105	Sensor	GesturePebbleZ1	132	172	6	Vary
106	Sensor	GesturePebbleZ2	146	158	6	Vary
107	Motion	GunPointAgeSpan	135	316	2	150
108	Motion	GunPointMaleVersusFemale	135	316	2	150
109	Motion	GunPointOldVersusYoung	136	315	2	150
110	Device	HouseTwenty	40	119	2	2000

111	EPG	InsectEPGRegularTrain	62	249	3	601
112	EPG	InsectEPGSmallTrain	17	249	3	601
113	Traffic	MelbournePedestrian	1194	2439	10	24
114	Image	MixedShapesRegularTrain	500	2425	5	1024
115	Image	MixedShapesSmallTrain	100	2425	5	1024
116	Sensor	PickupGestureWiimoteZ	50	50	10	Vary
117	Hemodynamics	PigAirwayPressure	104	208	52	2000
118	Hemodynamics	PigArtPressure	104	208	52	2000
119	Hemodynamics	PigCVP	104	208	52	2000
120	Device	PLAID	537	537	11	Vary
121	Power	PowerCons	180	180	2	144
122	Spectrum	Rock	20	50	4	2844
123	Spectrum	SemgHandGenderCh2	300	600	2	1500
124	Spectrum	SemgHandMovementCh2	450	450	6	1500
125	Spectrum	SemgHandSubjectCh2	450	450	5	1500
126	Sensor	ShakeGestureWiimoteZ	50	50	10	Vary
127	Simulated	SmoothSubspace	150	150	3	15
128	Simulated	UMD	36	144	3	150

A.2 Summary of UEA Multivariate Datasets

Table 4: Summary of UEA Multivariate Datasets

ID	Dataset	TrainSize	TestSize	NumDimensions	Class	Length
1	ArticularyWordRecognition	275	300	9	25	144
2	AtrialFibrillation	15	15	2	3	640
3	BasicMotions	40	40	6	4	100
4	CharacterTrajectories	1422	1436	3	20	182
5	Cricket	108	72	6	12	1197
6	DuckDuckGeese	50	50	1345	5	270
7	EigenWorms	128	131	6	5	17984
8	Epilepsy	137	138	3	4	206
9	EthanolConcentration	261	263	3	4	1751
10	ERing	30	270	4	6	65
11	FaceDetection	5890	3524	144	2	62
12	FingerMovements	316	100	28	2	50
13	HandMovementDirection	160	74	10	4	400
14	Handwriting	150	850	3	26	152
15	Heartbeat	204	205	61	2	405
16	InsectWingbeat	30000	20000	200	10	30
17	JapaneseVowels	270	370	12	9	29
18	Libras	180	180	2	15	45
19	LSST	2459	2466	6	14	36
20	MotorImagery	278	100	64	2	3000
21	NATOPS	180	180	24	6	51
22	PenDigits	7494	3498	2	10	8
23	PEMS-SF	267	173	963	7	144
24	Phoneme	3315	3353	11	39	217
25	RacketSports	151	152	6	4	30
26	SelfRegulationSCP1	268	293	6	2	896
27	SelfRegulationSCP2	200	180	7	2	1152
28	SpokenArabicDigits	6599	2199	13	10	93
29	StandWalkJump	12	15	4	3	2500
30	UWaveGestureLibrary	120	320	3	8	315

B Performance of UCR/UEA Datasets in Detail

Table 5: Classification Results of UCR Univariate Time Series Datasets

Dataset	Time2Image	InceptionTime	FCN	ResNet	GAF+ViT	MTF+ViT	RP+ViT	Time2Image-ResNet
ACSF1	82.60%	91.00%	85.20%	88.80%	14.00%	10.00%	36.00%	44.80%
Adiac	77.95%	84.40%	71.30%	84.81%	9.72%	3.07%	28.90%	72.58%
AllGestureWiimoteX	70.97%	-	10.00%	10.00%	-	-	-	59.57%
AllGestureWiimoteY	72.06%	-	10.00%	10.00%	-	-	-	65.20%
AllGestureWiimoteZ	65.29%	-	10.00%	10.00%	-	-	-	54.69%
ArrowHead	84.46%	86.29%	66.06%	83.09%	40.57%	39.43%	64.00%	54.74%
Beef	91.33%	66.67%	47.33%	64.00%	40.00%	33.33%	43.33%	52.80%
BeetleFly	99.00%	85.00%	78.00%	83.00%	75.00%	50.00%	95.00%	63.00%
BirdChicken	100.00%	95.00%	91.00%	93.00%	65.00%	50.00%	80.00%	74.00%
BME	100.00%	100.00%	56.40%	96.80%	50.67%	33.33%	52.67%	93.27%
Car	83.33%	90.00%	70.67%	92.33%	28.33%	23.33%	51.67%	60.36%
CBF	99.96%	99.89%	98.71%	99.62%	41.33%	33.11%	80.67%	77.27%
Chinatown	98.13%	98.54%	98.08%	98.02%	76.09%	72.59%	92.71%	79.77%
ChlorineConcentration	80.04%	87.60%	65.11%	84.28%	54.71%	53.26%	55.99%	56.92%
CinCECGTorso	77.88%	85.29%	70.29%	75.94%	42.46%	24.86%	95.07%	37.65%
Coffee	100.00%	100.00%	99.29%	100.00%	78.57%	53.57%	92.86%	77.14%
Computers	79.28%	80.80%	84.40%	83.68%	67.60%	50.80%	65.60%	68.64%
CricketX	79.95%	84.87%	74.46%	78.87%	14.62%	7.44%	62.56%	74.41%
CricketY	79.08%	84.36%	75.13%	80.56%	16.41%	7.95%	63.85%	75.23%
CricketZ	84.10%	84.87%	77.33%	80.87%	14.87%	7.18%	60.77%	75.64%
Crop	75.00%	79.85%	75.68%	76.81%	29.40%	4.17%	4.17%	75.24%
DiatomSizeReduction	98.37%	94.77%	79.28%	93.99%	46.08%	30.07%	54.25%	67.19%
DistalPhalanxOutlineAgeGroup	79.14%	73.38%	76.69%	72.95%	58.99%	46.76%	78.42%	77.41%
DistalPhalanxOutlineCorrect	81.59%	78.62%	76.88%	77.83%	63.77%	58.33%	75.36%	79.20%
DistalPhalanxTW	72.52%	65.47%	70.22%	68.49%	46.76%	30.22%	69.06%	73.67%
DodgerLoopDay	67.00%	-	15.75%	15.75%	-	-	-	65.75%
DodgerLoopGame	94.49%	-	51.30%	48.70%	-	-	-	61.30%
DodgerLoopWeekend	98.55%	-	54.78%	64.35%	-	-	-	87.39%
Earthquakes	78.71%	71.22%	72.52%	73.53%	76.98%	74.82%	74.82%	78.14%
ECG200	93.40%	91.00%	88.80%	86.80%	73.00%	64.00%	86.00%	87.68%
ECG5000	94.82%	94.16%	94.02%	93.91%	78.58%	58.38%	94.44%	88.18%
ECGFiveDays	91.87%	100.00%	93.64%	97.96%	67.94%	49.71%	79.67%	63.22%
ElectricDevices	76.86%	72.12%	74.69%	72.03%				69.93%

Table 5: Classification Results of UCR Univariate Time Series Datasets

Dataset	Time2Image	InceptionTime	FCN	ResNet	GAF+ViT	MTF+ViT	RP+ViT	Time2Image-ResNet
EOGHorizontalSignal	60.61%	62.98%	48.40%	64.36%	11.05%	8.56%	46.13%	58.17%
EOGVerticalSignal	55.36%	51.66%	37.29%	45.75%	9.39%	8.84%	41.44%	60.06%
EthanolLevel	65.16%	83.20%	42.20%	85.52%	25.80%	25.20%	29.80%	29.88%
FaceAll	74.72%	79.29%	91.01%	85.65%	28.82%	16.98%	79.41%	79.20%
FaceFour	88.41%	95.45%	75.91%	94.77%	27.27%	29.55%	61.36%	38.86%
FacesUCR	90.64%	97.22%	91.98%	94.73%	27.46%	14.34%	72.34%	87.44%
FiftyWords	79.12%	84.62%	53.49%	71.91%	23.52%	12.53%	66.59%	78.20%
Fish	90.17%	98.29%	90.63%	98.17%	29.71%	12.57%	53.14%	94.74%
FordA	93.98%	96.06%	91.89%	93.20%	-	-	-	94.97%
FordB	80.86%	84.94%	79.46%	81.14%	-	-	-	81.60%
FreezerRegularTrain	99.59%	99.68%	99.47%	99.82%	70.42%	50.00%	78.84%	91.24%
FreezerSmallTrain	90.89%	84.60%	74.89%	83.17%	62.28%	50.00%	78.14%	77.35%
Fungi	99.68%	-	78.06%	98.49%	13.98%	10.22%	74.19%	36.24%
GestureMidAirD1	72.77%	-	69.23%	68.00%	-	-	-	71.69%
GestureMidAirD2	66.46%	-	64.61%	67.00%	-	-	-	68.46%
GestureMidAirD3	40.46%	-	33.00%	34.00%	-	-	-	44.46%
GesturePebbleZ1	95.12%	-	15.70%	15.70%	-	-	-	90.93%
GesturePebbleZ2	85.82%	-	15.82%	15.82%	-	-	-	87.47%
GunPoint	99.60%	100.00%	99.33%	100.00%	72.00%	50.67%	77.33%	65.60%
GunPointAgeSpan	98.73%	99.05%	90.57%	99.37%	73.42%	50.63%	99.05%	96.90%
GunPointMaleVersusFemale	99.81%	100.00%	99.81%	99.49%	69.94%	52.53%	99.68%	99.18%
GunPointOldVersusYoung	99.49%	100.00%	100.00%	100.00%	59.37%	52.38%	100.00%	89.24%
Ham	79.43%	72.38%	73.71%	75.43%	57.14%	51.43%	62.86%	69.71%
HandOutlines	92.86%	95.95%	77.35%	92.97%	66.22%	64.05%	92.16%	92.38%
Haptics	50.97%	57.14%	42.79%	53.25%	20.78%	20.78%	43.83%	30.91%
Herring	70.00%	70.31%	64.37%	65.63%	59.38%	59.38%	59.38%	60.63%
HouseTwenty	95.46%	91.60%	91.93%	95.29%	65.55%	57.98%	88.24%	79.16%
InlineSkate	40.58%	48.55%	35.89%	46.40%	16.36%	16.36%	26.18%	27.13%
InsectEPGRegularTrain	100.00%	100.00%	100.00%	100.00%	81.12%	47.39%	47.39%	86.43%
InsectEPGSmallTrain	99.52%	100.00%	100.00%	100.00%	67.87%	47.39%	47.39%	83.21%
InsectWingbeatSound	59.80%	63.69%	40.90%	50.31%	19.65%	9.19%	58.23%	62.21%
ItalyPowerDemand	96.85%	96.60%	95.86%	95.72%	68.80%	50.15%	96.02%	85.15%
LargeKitchenAppliances	85.55%	90.40%	89.76%	90.08%	48.53%	34.40%	74.67%	75.31%

Table 5: Classification Results of UCR Univariate Time Series Datasets

Dataset	Time2Image	InceptionTime	FCN	ResNet	GAF+ViT	MTF+ViT	RP+ViT	Time2Image-ResNet
Lightning2	85.25%	83.61%	71.48%	75.74%	-	-	-	79.67%
Lightning7	83.84%	79.45%	71.78%	80.00%	36.99%	26.03%	65.75%	75.89%
Mallat	93.93%	95.78%	72.95%	96.34%	12.41%	12.41%	52.79%	73.09%
Meat	92.67%	95.00%	75.00%	93.33%	41.67%	33.33%	71.67%	42.33%
MedicalImages	78.16%	79.61%	77.45%	77.74%	52.50%	51.45%	72.24%	70.47%
MelbournePedestrian	90.59%	-	10.05%	10.05%	-	-	-	91.63%
MiddlePhalanxOutlineAgeGroup	66.75%	55.19%	59.74%	54.42%	43.51%	18.83%	63.64%	65.71%
MiddlePhalanxOutlineCorrect	82.41%	83.51%	82.34%	81.51%	63.57%	57.04%	68.38%	67.56%
MiddlePhalanxTW	64.29%	53.25%	55.19%	48.57%	46.75%	27.27%	61.04%	61.82%
MixedShapesRegularTrain	92.92%	97.03%	94.93%	97.68%	26.97%	26.97%	90.89%	90.92%
MixedShapesSmallTrain	85.76%	91.09%	87.92%	92.29%	26.97%	26.97%	79.18%	83.99%
MoteStrain	91.82%	89.38%	91.63%	92.16%	59.82%	54.95%	82.35%	71.90%
NonInvasiveFetalECGThorax1	94.14%	95.83%	89.97%	96.04%	11.40%	2.34%	84.89%	92.73%
NonInvasiveFetalECGThorax2	94.05%	95.88%	91.09%	95.29%	26.46%	2.34%	89.67%	93.82%
OliveOil	74.67%	86.67%	40.00%	62.00%	40.00%	40.00%	40.00%	44.66%
OSULeaf	76.20%	92.15%	97.27%	98.43%	26.03%	18.18%	77.27%	58.08%
PhalangesOutlinesCorrect	83.85%	85.20%	80.82%	82.73%	62.94%	61.31%	67.72%	80.11%
Phoneme	26.34%	33.70%	32.75%	35.31%	11.29%	11.29%	19.78%	30.58%
PickupGestureWiimoteZ	72.40%	-	10.00%	10.00%	-	-	-	48.16%
PigAirwayPressure	23.94%	94.23%	31.15%	67.50%	3.37%	1.92%	8.65%	24.96%
PigArtPressure	72.12%	100.00%	58.27%	99.52%	2.40%	1.92%	61.06%	43.75%
PigCVP	69.04%	96.63%	20.48%	21.35%	1.92%	1.92%	16.35%	41.15%
PLAID	81.53%	-	16.20%	16.20%	-	-	-	71.98%
Plane	100.00%	100.00%	100.00%	100.00%	43.81%	9.52%	100.00%	99.43%
PowerCons	98.22%	99.44%	90.00%	88.89%	86.67%	50.00%	95.00%	97.00%
ProximalPhalanxOutlineAgeGroup	88.10%	84.88%	84.68%	84.19%	69.27%	85.37%	87.80%	88.59%
ProximalPhalanxOutlineCorrect	83.37%	93.13%	89.35%	90.93%	69.42%	68.38%	83.85%	87.35%
ProximalPhalanxTW	83.02%	80.00%	81.07%	77.56%	56.59%	35.12%	81.46%	81.95%
RefrigerationDevices	56.11%	51.47%	52.37%	52.32%	49.33%	33.87%	56.00%	57.17%
Rock	79.20%	60.00%	31.60%	55.20%	42.00%	42.00%	80.00%	49.20%
ScreenType	52.21%	59.47%	63.57%	63.31%	45.07%	33.60%	42.67%	46.29%
SemgHandGenderCh2	90.80%	87.33%	80.77%	83.77%	65.00%	65.00%	94.17%	89.87%
SemgHandMovementCh2	64.67%	58.44%	44.00%	50.62%	16.67%	16.67%	72.67%	50.36%

Table 5: Classification Results of UCR Univariate Time Series Datasets

Dataset	Time2Image	InceptionTime	FCN	ResNet	GAF+ViT	MTF+ViT	RP+ViT	Time2Image-ResNet
SemgHandSubjectCh2	84.89%	73.33%	53.38%	59.51%	20.00%	20.00%	92.89%	81.16%
ShakeGestureWiimoteZ	93.20%	-	10.00%	10.00%	-	-	-	45.60%
ShapeletSim	67.11%	99.44%	99.22%	95.11%	96.67%	50.00%	62.78%	54.22%
ShapesAll	85.33%	92.50%	80.90%	90.63%	12.83%	1.67%	71.17%	83.07%
SmallKitchenAppliances	74.03%	77.87%	80.11%	78.72%	53.33%	34.13%	70.40%	75.41%
SmoothSubspace	99.33%	98.00%	99.47%	98.67%	55.33%	37.33%	33.33%	98.67%
SonyAIBORobotSurface1	92.18%	87.85%	95.61%	93.41%	49.25%	42.93%	95.51%	64.66%
SonyAIBORobotSurface2	94.19%	95.17%	97.33%	98.11%	65.90%	61.70%	80.06%	74.14%
StarLightCurves	97.56%	97.84%	97.22%	97.44%	72.30%	57.72%	96.95%	97.18%
Strawberry	97.41%	98.38%	96.16%	97.62%	71.08%	64.32%	94.86%	97.30%
SwedishLeaf	92.74%	96.96%	95.97%	96.06%	22.40%	5.28%	90.24%	91.90%
Symbols	93.05%	98.49%	82.93%	96.34%	39.20%	17.39%	52.66%	78.83%
SyntheticControl	99.93%	99.67%	98.33%	99.80%	31.00%	16.67%	66.67%	99.33%
ToeSegmentation1	95.26%	96.49%	95.79%	96.14%	54.82%	52.63%	74.56%	80.70%
ToeSegmentation2	92.46%	94.62%	91.38%	89.23%	82.31%	81.54%	90.77%	87.38%
Trace	100.00%	100.00%	100.00%	100.00%	56.00%	19.00%	78.00%	96.60%
TwoLeadECG	99.72%	99.56%	99.93%	99.89%	58.21%	50.04%	67.52%	63.51%
TwoPatterns	100.00%	100.00%	85.97%	99.90%	41.43%	25.88%	51.13%	100.00%
UMD	99.03%	98.61%	99.31%	98.89%	48.61%	33.33%	52.78%	89.86%
UWaveGestureLibraryAll	96.90%	95.09%	79.97%	86.74%	25.43%	12.53%	90.87%	96.71%
UWaveGestureLibraryX	82.57%	82.22%	77.84%	78.71%	25.54%	12.53%	64.32%	81.38%
UWaveGestureLibraryY	74.33%	77.14%	66.59%	68.34%	27.44%	18.45%	66.16%	72.16%
UWaveGestureLibraryZ	76.33%	76.86%	74.38%	76.24%	27.83%	12.20%	67.09%	74.47%
Wafer	99.68%	99.87%	99.67%	99.89%	92.94%	89.21%	99.66%	99.64%
Wine	76.67%	62.96%	60.74%	71.11%	59.26%	50.00%	55.56%	51.11%
WordSynonyms	69.72%	74.45%	45.58%	58.40%	29.15%	21.94%	54.08%	68.37%
Worms	64.68%	80.52%	69.09%	81.04%	61.04%	42.86%	63.64%	62.86%
WormsTwoClass	78.96%	76.62%	76.10%	77.14%	64.94%	57.14%	79.22%	65.71%
Yoga	86.80%	90.50%	75.17%	87.17%	55.37%	53.57%	76.93%	77.60%
Average accuracy	87.76%	88.84%	81.12%	84.25%	49.17%	36.90%	73.44%	79.07%

Table 6: Classification Results of UEA Multivariate Time Series Datasets

Dataset	Time2Image	ROCKET	CIF	HIVE-COTE	ResNet	InceptionTime	Time2Image+ResNet
ArticularyWordRecognition	97.80%	99.56%	97.89%	97.99%	98.26%	99.10%	94.33%
AtrialFibrillation	45.33%	24.89%	25.11%	25.11%	36.22%	22.00%	53.33%
BasicMotions	99.00%	99.00%	99.75%	100.00%	100.00%	100.00%	58.50%
CharacterTrajectories	99.50%	-	-	-	-	-	99.25%
Cricket	100.00%	100.00%	98.38%	99.26%	99.40%	99.44%	90.83%
DuckDuckGeese	47.20%	46.13%	56.00%	47.60%	63.20%	63.47%	47.60%
ERing	89.93%	86.28%	90.33%	78.17%	45.45%	-	44.12%
EigenWorms	79.24%	99.08%	98.38%	100.00%	99.18%	98.65%	74.06%
Epilepsy	96.09%	44.68%	72.89%	80.68%	28.66%	27.92%	26.31%
EthanolConcentration	28.67%	98.05%	95.65%	94.26%	87.19%	92.10%	55.48%
FaceDetection	67.79%	69.42%	68.89%	69.17%	62.97%	77.24%	50.04%
FingerMovements	58.00%	55.27%	53.90%	53.77%	54.70%	56.13%	55.00%
HandMovementDirection	61.89%	44.59%	52.21%	37.79%	35.32%	42.39%	41.08%
Handwriting	44.80%	56.67%	35.13%	50.41%	59.78%	65.74%	16.05%
Heartbeat	75.61%	71.76%	76.52%	72.18%	63.89%	73.20%	72.59%
InsectWingbeat	47.60%	-	-	-	-	-	52.97%
JapaneseVowels	89.51%	-	-	-	-	-	83.30%
LSST	65.24%	90.61%	91.67%	90.28%	94.11%	88.72%	79.89%
Libras	86.44%	63.15%	56.17%	53.84%	42.94%	33.97%	61.01%
MotorImagery	63.60%	53.13%	51.80%	52.17%	49.77%	51.17%	55.40%
NATOPS	86.33%	88.54%	84.41%	82.85%	97.11%	96.63%	78.11%
PEMS-SF	84.62%	99.56%	98.97%	97.19%	99.64%	99.68%	99.05%
PenDigits	99.11%	85.63%	99.85%	97.98%	81.95%	82.83%	77.11%
PhonemeSpectra	24.94%	28.35%	26.56%	32.87%	30.86%	36.74%	23.08%
RacketSports	89.87%	92.79%	89.30%	90.64%	94.23%	91.69%	73.03%
SelfRegulationSCP1	85.94%	86.55%	85.94%	86.02%	76.11%	84.69%	86.14%
SelfRegulationSCP2	60.22%	51.35%	48.87%	51.67%	50.24%	52.04%	52.11%
SpokenArabicDigits	99.41%	-	-	-	-	-	99.32%
StandWalkJump	66.67%	45.56%	45.11%	40.67%	30.89%	42.00%	66.67%
UWaveGestureLibrary	89.31%	94.43%	92.42%	91.31%	88.35%	91.23%	80.31%
Average accuracy	74.32%	72.12%	72.77%	72.07%	68.09%	70.75%	64.87%

C PARAMETER ANALYSIS

Table 7: Parameter Analysis of UCR/UEA Archive

Dataset	σ=R	σ=R/2	σ=R/3	Difference	Variance
ArticularyWordRecognition	97.0000%	97.8000%	97.6667%	0.8000%	0.0018%
AtrialFibrillation	40.0000%	45.3333%	40.0000%	5.3333%	0.0948%
BasicMotions	97.5000%	99.0000%	97.5000%	1.5000%	0.0075%
CharacterTrajectories	99.3036%	99.4986%	99.5125%	0.2089%	0.0001%
Cricket	98.6111%	100.0000%	98.6111%	1.3889%	0.0064%
DuckDuckGeese	52.0000%	47.2000%	46.0000%	6.0000%	0.1008%
EigenWorms	77.8626%	89.9259%	78.6260%	12.0633%	0.4563%
Epilepsy	94.9275%	79.2366%	97.1015%	17.8648%	0.9501%
EthanolConcentration	28.8973%	96.0870%	31.5589%	67.1896%	14.4757%
ERing	87.0370%	28.6692%	94.0741%	65.4049%	12.8902%
FaceDetection	67.2247%	67.7923%	67.7639%	0.5675%	0.0010%
FingerMovements	61.0000%	58.0000%	59.0000%	3.0000%	0.0233%
HandMovementDirection	50.0000%	61.8919%	60.8108%	11.8919%	0.4324%
Handwriting	42.3529%	44.8000%	45.4118%	3.0588%	0.0262%
Heartbeat	75.1220%	75.6098%	76.0976%	0.9756%	0.0024%
InsectWingbeat	47.1480%	47.6024%	47.5600%	0.4544%	0.0006%
JapaneseVowels	91.6216%	89.5135%	91.8919%	2.3784%	0.0170%
Libras	86.1111%	65.2393%	88.3333%	23.0941%	1.6232%
LSST	64.8824%	86.4444%	65.5312%	21.5620%	1.5045%
MotorImagery	60.0000%	63.6000%	62.0000%	3.6000%	0.0325%
NATOPS	85.0000%	86.3333%	87.7778%	2.7778%	0.0193%
PenDigits	98.7707%	84.6243%	99.2281%	14.6039%	0.6893%
PEMS-SF	86.7052%	99.1138%	84.3931%	14.7207%	0.6267%
PhonemeSpectra	26.0960%	24.9389%	25.4399%	1.1572%	0.0034%
RacketSports	90.1316%	89.8684%	88.1579%	1.9737%	0.0115%
SelfRegulationSCP1	87.0307%	85.9386%	86.0068%	1.0921%	0.0037%
SelfRegulationSCP2	60.0000%	60.2222%	55.0000%	5.2222%	0.0872%
SpokenArabicDigits	99.4543%	99.4088%	99.3633%	0.0910%	0.0000%
StandWalkJump	73.3333%	66.6667%	80.0000%	13.3333%	0.4444%
UWaveGestureLibrary	90.0000%	89.3125%	90.3125%	1.0000%	0.0026%
ACSF1	74.0000%	82.6000%	80.0000%	8.6000%	0.1945%
Adiac	69.8210%	77.9540%	77.2379%	8.1330%	0.2028%
AllGestureWiimoteX	72.7143%	70.9714%	72.5714%	1.7429%	0.0094%
AllGestureWiimoteY	71.7143%	72.0571%	72.0000%	0.3429%	0.0003%
AllGestureWiimoteZ	63.2857%	65.2857%	65.2857%	2.0000%	0.0133%
ArrowHead	82.2857%	84.4571%	82.8571%	2.1714%	0.0127%
Beef	90.0000%	91.3333%	90.0000%	1.3333%	0.0059%
BeetleFly	95.0000%	99.0000%	100.0000%	5.0000%	0.0700%
BirdChicken	100.0000%	100.0000%	100.0000%	0.0000%	0.0000%
BME	100.0000%	100.0000%	100.0000%	0.0000%	0.0000%
Car	75.0000%	83.3333%	85.0000%	10.0000%	0.2870%
CBF	99.6667%	99.9556%	100.0000%	0.3333%	0.0003%
Chinatown	98.8338%	98.1341%	97.9592%	0.8746%	0.0021%
ChlorineConcentration	68.9323%	80.0365%	81.1719%	12.2396%	0.4573%
CinCECGTorso	78.7681%	77.8841%	70.9420%	7.8261%	0.1837%
Coffee	100.0000%	100.0000%	100.0000%	0.0000%	0.0000%
Computers	76.4000%	79.2800%	77.2000%	2.8800%	0.0221%
CricketX	80.5128%	79.9487%	82.0513%	2.1026%	0.0118%
CricketY	79.7436%	79.0769%	77.6923%	2.0513%	0.0109%
CricketZ	84.6154%	84.1026%	83.8462%	0.7692%	0.0015%
Crop	74.8869%	74.9952%	74.2381%	0.7571%	0.0017%
DiatomSizeReduction	88.5621%	98.3660%	98.3660%	9.8039%	0.3204%
DistalPhalanxOutlineAgeGroup	76.2590%	79.1367%	78.4173%	2.8777%	0.0224%

Table 7 continued from previous page

Dataset	σ=R	σ=R/2	σ=R/3	Difference	Variance
DistalPhalanxOutlineCorrect	80.7971%	81.5942%	81.5217%	0.7971%	0.0019%
DistalPhalanxTW	72.6619%	72.5180%	71.9424%	0.7194%	0.0014%
DodgerLoopDay	63.7500%	67.0000%	65.0000%	3.2500%	0.0269%
DodgerLoopGame	94.2029%	94.4928%	94.2029%	0.2899%	0.0003%
DodgerLoopWeekend	97.8261%	98.5507%	97.8261%	0.7246%	0.0018%
Earthquakes	76.9784%	78.7050%	77.6978%	1.7266%	0.0075%
ECG200	93.0000%	93.4000%	92.0000%	1.4000%	0.0052%
ECG5000	94.3778%	94.8222%	94.8222%	0.4444%	0.0007%
ECGFiveDays	92.9152%	91.8699%	95.5865%	3.7166%	0.0367%
ElectricDevices	76.7864%	76.8590%	76.1769%	0.6821%	0.0014%
EOGHorizontalSignal	58.2873%	60.6077%	61.6022%	3.3149%	0.0289%
EOGVerticalSignal	55.5249%	55.3591%	55.5249%	0.1657%	0.0001%
EthanolLevel	30.8000%	65.1600%	76.0000%	45.2000%	5.5686%
FaceAll	76.3905%	74.7219%	74.6746%	1.7160%	0.0096%
FaceFour	85.2273%	88.4091%	89.7727%	4.5455%	0.0544%
FacesUCR	90.4878%	90.6439%	89.4146%	1.2293%	0.0045%
FiftyWords	78.9011%	79.1209%	80.0000%	1.0989%	0.0034%
Fish	86.2857%	90.1714%	92.5714%	6.2857%	0.1006%
FordA	94.0909%	93.9848%	93.8636%	0.2273%	0.0001%
FordB	79.7531%	80.8642%	81.4815%	1.7284%	0.0077%
FreezerRegularTrain	99.6842%	99.5860%	99.4386%	0.2456%	0.0002%
FreezerSmallTrain	88.3860%	90.8912%	87.2281%	3.6632%	0.0351%
Fungi	80.1075%	99.6774%	100.0000%	19.8925%	1.2980%
GestureMidAirD1	76.1538%	72.7692%	72.3077%	3.8462%	0.0441%
GestureMidAirD2	66.9231%	66.4615%	67.6923%	1.2308%	0.0039%
GestureMidAirD3	40.7692%	40.4615%	41.5385%	1.0769%	0.0031%
GesturePebbleZ1	95.9302%	95.1163%	95.3488%	0.8140%	0.0018%
GesturePebbleZ2	86.7089%	85.8228%	87.3418%	1.5190%	0.0058%
GunPoint	100.0000%	99.6000%	97.3333%	2.6667%	0.0207%
GunPointAgeSpan	98.4177%	98.7342%	98.7342%	0.3165%	0.0003%
GunPointMaleVersusFemale	99.6835%	99.8101%	99.6835%	0.1266%	0.0001%
GunPointOldVersusYoung	99.0476%	99.4921%	100.0000%	0.9524%	0.0023%
Ham	80.9524%	79.4286%	80.9524%	1.5238%	0.0077%
HandOutlines	92.1622%	92.8649%	92.9730%	0.8108%	0.0019%
Haptics	49.0260%	50.9740%	51.6234%	2.5974%	0.0183%
Herring	65.6250%	70.0000%	67.1875%	4.3750%	0.0492%
HouseTwenty	94.9580%	95.4622%	94.9580%	0.5042%	0.0008%
InlineSkate	39.6364%	40.5818%	40.0000%	0.9455%	0.0023%
InsectEPGRegularTrain	100.0000%	100.0000%	100.0000%	0.0000%	0.0000%
InsectEPGSmallTrain	99.5984%	99.5181%	99.5984%	0.0803%	0.0000%
InsectWingbeatSound	59.3434%	59.7980%	60.5051%	1.1616%	0.0034%
ItalyPowerDemand	96.6958%	96.8513%	96.8902%	0.1944%	0.0001%
LargeKitchenAppliances	84.5333%	85.5467%	84.8000%	1.0133%	0.0028%
Lightning2	86.8852%	85.2459%	85.2459%	1.6393%	0.0090%
Lightning7	82.1918%	83.8356%	84.9315%	2.7397%	0.0190%
Mallat	93.2196%	93.9275%	95.8635%	2.6439%	0.0187%
Meat	88.3333%	92.6667%	88.3333%	4.3333%	0.0626%
MedicalImages	77.8947%	78.1579%	76.4474%	1.7105%	0.0085%
MelbournePedestrian	91.9639%	90.5945%	90.8569%	1.3694%	0.0053%
MiddlePhalanxOutlineAgeGroup	66.8831%	66.7532%	66.8831%	0.1299%	0.0001%
MiddlePhalanxOutlineCorrect	85.2234%	82.4055%	81.4433%	3.7801%	0.0386%
MiddlePhalanxTW	63.6364%	64.2857%	64.2857%	0.6494%	0.0014%
MixedShapesRegularTrain	93.5258%	92.9155%	92.8660%	0.6598%	0.0014%
MixedShapesSmallTrain	86.7216%	85.7567%	34.3918%	52.3299%	8.9628%
MoteStrain	88.4984%	91.8211%	93.0511%	4.5527%	0.0555%
NonInvasiveFetalECGThorax1	93.1807%	94.1374%	93.5369%	0.9567%	0.0023%
NonInvasiveFetalECGThorax2	94.1985%	94.0458%	93.9949%	0.2036%	0.0001%

Table 7 continued from previous page

Dataset	σ=R	σ=R/2	σ=R/3	Difference	Variance
OliveOil	73.3333%	74.6667%	80.0000%	6.6667%	0.1244%
OSULeaf	75.6198%	76.1983%	74.7934%	1.4050%	0.0050%
PhalangesOutlinesCorrect	83.6830%	83.8462%	84.7319%	1.0490%	0.0032%
Phoneme	24.5781%	26.3397%	27.0042%	2.4262%	0.0157%
PickupGestureWiimoteZ	74.0000%	72.4000%	78.0000%	5.6000%	0.0832%
PigAirwayPressure	13.9423%	23.9423%	24.5192%	10.5769%	0.3537%
PigArtPressure	53.3654%	72.1154%	74.0385%	20.6731%	1.3044%
PigCVP	61.5385%	69.0385%	71.1538%	9.6154%	0.2553%
PLAID	80.4469%	81.5270%	82.1229%	1.6760%	0.0072%
Plane	100.0000%	100.0000%	100.0000%	0.0000%	0.0000%
PowerCons	98.8889%	98.2222%	97.7778%	1.1111%	0.0031%
ProximalPhalanxOutlineAgeGroup	87.8049%	88.0976%	87.8049%	0.2927%	0.0003%
ProximalPhalanxOutlineCorrect	82.1306%	83.3677%	82.8179%	1.2371%	0.0038%
ProximalPhalanxTW	82.9268%	83.0244%	83.9024%	0.9756%	0.0029%
RefrigerationDevices	55.7333%	56.1067%	56.8000%	1.0667%	0.0029%
Rock	74.0000%	79.2000%	74.0000%	5.2000%	0.0901%
ScreenType	54.6667%	52.2133%	52.2667%	2.4533%	0.0196%
SemgHandGenderCh2	91.3333%	90.8000%	90.8333%	0.5333%	0.0009%
SemgHandMovementCh2	65.1111%	64.6667%	64.2222%	0.8889%	0.0020%
SemgHandSubjectCh2	86.4444%	84.8889%	84.6667%	1.7778%	0.0094%
ShakeGestureWiimoteZ	94.0000%	93.2000%	92.0000%	2.0000%	0.0101%
ShapeletSim	66.1111%	67.1111%	64.4444%	2.6667%	0.0181%
ShapesAll	84.8333%	85.3333%	86.5000%	1.6667%	0.0073%
SmallKitchenAppliances	74.9333%	74.0267%	72.8000%	2.1333%	0.0115%
SmoothSubspace	98.6667%	99.3333%	100.0000%	1.3333%	0.0044%
SonyAIBORobotSurface1	92.1797%	92.1797%	92.1797%	0.0000%	0.0000%
SonyAIBORobotSurface2	90.4512%	94.1868%	93.4942%	3.7356%	0.0395%
StarLightCurves	97.2317%	97.5619%	97.6688%	0.4371%	0.0005%
Strawberry	97.0270%	97.4054%	97.5676%	0.5405%	0.0008%
SwedishLeaf	92.9600%	92.7360%	91.8400%	1.1200%	0.0035%
Symbols	88.6432%	93.0452%	95.6784%	7.0352%	0.1263%
SyntheticControl	99.3333%	99.9333%	99.6667%	0.6000%	0.0009%
ToeSegmentation1	93.4211%	95.2632%	93.8596%	1.8421%	0.0093%
ToeSegmentation2	91.5385%	92.4615%	93.0769%	1.5385%	0.0060%
Trace	100.0000%	100.0000%	100.0000%	0.0000%	0.0000%
TwoLeadECG	99.6488%	99.7191%	99.7366%	0.0878%	0.0000%
TwoPatterns	100.0000%	100.0000%	100.0000%	0.0000%	0.0000%
UMD	98.6111%	99.0278%	99.3056%	0.6944%	0.0012%
UWaveGestureLibraryAll	97.2641%	96.9012%	96.9570%	0.3629%	0.0004%
UWaveGestureLibraryX	82.4400%	82.5684%	83.1658%	0.7259%	0.0015%
UWaveGestureLibraryY	74.3439%	74.3272%	74.1485%	0.1954%	0.0001%
UWaveGestureLibraryZ	75.6561%	76.3261%	76.8007%	1.1446%	0.0033%
Wafer	99.6106%	99.6820%	99.7404%	0.1298%	0.0000%
Wine	50.0000%	76.6667%	75.9259%	26.6667%	2.3064%
WordSynonyms	70.0627%	69.7179%	68.6520%	1.4107%	0.0054%
Worms	71.4286%	64.6753%	66.2338%	6.7532%	0.1250%
WormsTwoClass	74.0260%	78.9610%	83.1169%	9.0909%	0.2071%
Yoga	87.4333%	86.8000%	86.7000%	0.7333%	0.0016%